iJRASET
International Journal For Research in Applied Science and Engineering Technology

INTERNATIONAL JOURNAL FOR RESEARCH

IN APPLIED SCIENCE & ENGINEERING TECHNOLOGY

Volume: 6 **Issue:** II **Month of publication:** February 2018

DOI: http://doi.org/10.22214/ijraset.2018.2095

www.ijraset.com

Call: 08813907089 | E-mail ID: ijraset@gmail.com

International Journal for Research in Applied Science & Engineering Technology (IJRASET)
ISSN: 2321-9653; IC Value: 45.98; SJ Impact Factor: 6.887
Volume 6 Issue II, February 2018- Available at www.ijraset.com

Electrical Characterization of SnO_2 based thick film resistors loaded with an optimized Sb: Sn alloy

B. R. Sharma[1], S U Shinde[2], N. D. Chaudhari[3]
[1,2,3]*Dept. of Physics Pratishthan Mahavidyalaya Paithan, Dist Aurangabad, M.S.*

Abstract: ***Thick Film Resistors (TFRs) are extensively being used in hybrid electronic technology, wherein high standards of electrical parameters and stability in changing thermal environment are required especially in space-research based industries. In the present paper, the optimized alloy $Sb_{0.6}$:$Sn_{0.4}$ of 5-10μm size was loaded in SnO_2nano-sized powder synthesized by sol-gel method, to produce range of resistive pastes. Thick Film Resistors fabrication and their electrical and material characterization using XRD and SEM studies have been reported. The fall in sheet resistivity ρ_s against loading fraction of optimized alloy $Sb_{0.6}$:$Sn_{0.4}$ in SnO_2nano-sized particles has been examined using percolation/effective medium theory.***

Keywords: Thick film resistor, Sheet Resistivity, TCR, Firing Temperature.

I. INTRODUCTION

The hybrid microelectronic thick film technology has been extensively used wherein the screen printed films are fired at high temperature can be used as planar passive components, such as, resistors, capacitors, conducting terminations etc. However thick film pastes/inks are based on expensive noble metals like Ru, RuO_2, Pd, gold, etc. The Thick Film Resistors (TFRs) are superior in performance, such as stability against load, low thermal noise, high current carrying capacity, non-inductive in nature, could be used at high frequencies[1-3].The cost effective SnO_2nanoparticles can be easily synthesized by sol-gel method, may be used as a functional material in the composition of TFR pastes[4-6]. S.H. Bhide et al used antimony as a dopent (5% by weight) in SnO_2 and reported sheet resistivity of 1MΩ/□and temperature coefficient of resistance (TCR) about -2000 PPM/ ºC [7]. M. R. Kadam et al reported that the film resistive pastes using SnO_2 as a functional material and loaded by $SnCl_2$ gives the minimum sheet resistance as ρ_s= 5 KΩ/□and TCR (α) as low as -950 ppm/°c and the paste containing SnO_2 : (Sb 5%) loaded by $SnCl_2$ resulted in the range of various resistive pastes[8]. Further Kattimani et al reported when Sb:Sn alloy loaded in SnO_2results in sudden fall in sheet resistivity at 5 % of Sb:Sn doping from 10^{12} Ω/□ to 750 Ω/□ followed by continuous steady decrease of resistivity and TCR at 90 % Sb:Sn alloy loading at 170 Ω/□ and TCR about -950 ppm/°c[9]. The research in nanoparticle physics is of interest due to high sensitivity for hydrogen, humidity, and LPG gas sensors[4-6,10].It is interesting to study electrical properties in the variation of optimized $Sb_{0.6}$:$Sn_{0.4}$ alloy of 5μm size loaded in SnO_2nano-sized particles as cost effective thick film resistors. The fall in resistivity over the whole range of weight fraction $W_m$in SnO_2 based thick films is predicted/expected to be similar to B. E. Springette's percolation model based on conducting particles mixed in uniform dielectric matrix[11].

II. EXPERIMENTAL PROCEDURE

A. Synthesis of SnO_2 and Sb:Sn Alloy

The Stannous Oxide (SnO_2) nano-sized particles were synthesized using standard sol-gel technique. The $SnC1_4.5H_20$ (AR grade) was dissolved in distilled water to make a 0.1 M solution. The prepared solution of $SnC1_4$ and H_20 was mixed with ammonia (NH_4OH, AR grade). The resulting precipitation was washed thoroughly with distilled water for longer times to remove excess ($C1^-$ and NH_4^+) Ions. The filtered resulting milky-white cake / gel were dried for 24 hrs at 100 °C under the IR lamp. The dried precipitate was ground into fine powder using agate mortar pestle and filtered through a 250 meshsize nylon cloth. The resulting powder was sintered/ calcined for 4hrs at various temperatures (500-1100 °C) to obtainSnO_2fine particles of various sizes ranging from 28-50 nm[4].Fine powders of antimony(Sb) and tin(Sn), both in particle size 5-10μm are weighed in different proportions (20:80,40:60,50:50,60:40,80:20) and are thoroughly mixed in acetone medium by using ball mill for 12 hrs. The quartz tubes are used and vacuum sealed by LPG and Oxygen torch in blue-white flame after filling the dried cake/alloy powder at 10^{-5}torr using rotary-diffusion pump. The sealed tubes are heated to 630 °C in a resistive furnace for 3 hrs. Then after slowly cooled alloy is

removed/collected by breaking quarts tubes and crushed in agate mortar pestle and ball milled for 12 hrs in acetone medium, dried under IR lamp then filtered through 250 mesh nylon cloth, ready to mix in SnO_2 to formulate the paste and TFRs.

B. Preparation of SnO_2 based Sb:Snalloy thick film Resistors

The Stannic oxide fine powder prepared by the above method was used as the basic functional material. The SnO_2based on optimized $Sb_{0.6}$:$Sn_{0.4}$ alloy paste was prepared with 10 % of standard lead borosilicate glass frit as a permanent or inorganic binder; ethyl cellulose (EC) and butyl carbitol acetate (BCA), were added suitably (solid to liquid ratio 70:30 by weight) so as temporary binder to get a thixotropic and rheological paste[12]. The paste was then screen printed on pure alumina (Al_2O_3) substrate (1˝× ½˝), dried for 4 hrs then firedat 800°C using induction heating for 45 minutes. For good electrical contact Silver electrodes were printed and dried under IR lamp after firing the films. The film thickness, as measured by light section microscope (BK 70 × 50Carl Zeiss, Jena) with an accuracy of ±0.5 µm, varies from 20 to 30µm and it is normalized to 1 mil or 25µm. The d.c. resistance of the pattern with different aspect ratios (N = L/W = 1, 1.5, 2) was measured by digital electrometer (Keithley EA-614). The time-temperature profile of the induction furnace was chosen so as to give good adhesion of uniform thick film formulation without any blisters or holes. The thickness of the thick films were monitored by light section microscope and ρ_s is normalized to 25 µm thickness used to measure sheet resistivity defined by

$$\rho_S = \frac{\rho_B}{t} = \frac{R}{N} = \frac{R \cdot W}{L} \qquad (1)$$

in the units of Ω/□. Where, ρ_B, R, t and N are the values of bulk resistivity, resistance, thickness and the aspect ratio (N = L/W = length/width) for the thick film resistor test pattern respectively. Resistor test pattern is having length L and width W for different values of N.

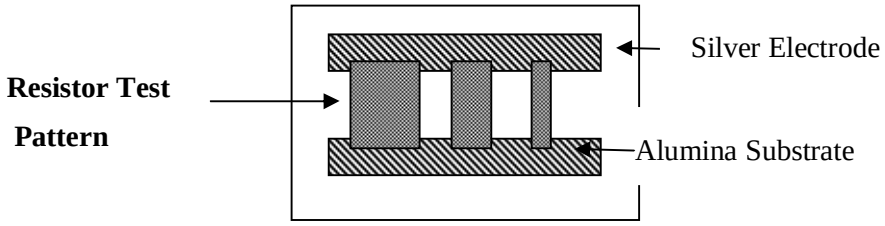

Fig. 1.Schematic representation of resistor test pattern on alumina substrate.

The temperature coefficient of resistance (TCR) is given by,

$$\alpha = \frac{1}{R(T)}\frac{dR(T)}{dT} = \frac{(R_1 - R_2)}{(R_2 \cdot T_1 - R_1 \cdot T_2)} \cdot 10^6 \; ppm/\,^\circ c \qquad (2)$$

Where, R_1 and R_2 are the values of resistors at the absolute temperatures T_1 and T_2 in linear region over R-T Characteristics in the range 30-130°C. The temperatures are monitored by temperature controller, based on alumel-chromel thermocouple using small resistive furnace.

C. X-ray analysis and Particle Size

The material characterization of TFRs was performed using X-ray diffraction and SEM techniques. Tin oxide occurs in various phases: orthorhombic, tetragonal, cubic or triclinic. But here only the tetragonal phase was revealed in x-ray analysis[13].X-ray diffraction analysis of tin oxide powder calcined at various temperatures500-1100 °C, as well as alloy powders made into thick films (suitable for resistors) was carried out using Philips PW-1840 diffractometer. Standard CuK_α radiation line having wavelength λ = 0.1542 nm was used as the X-ray source. The higher peak intensities of XRD pattern analysis reveals polycrystalline nature due to bigger grain size in the agglomerates of all the thick film resistors. Particle size analysis was made using the FWHM (β) width of the prominent diffraction peak and using the Debye-Scherrer formula,

$$D_{hkl} = 0.9\lambda/\beta \cos\theta \qquad (3)$$

Where D_{hkl} is the diameter of the particles in the hkl direction,λ is the X-ray wavelength of source and β is the full angular width of the diffraction peak at half the maximum intensity for diffraction angle 2θ in radians. From the Fig. 2, it is observed that the particle size D in the range 28-52 nm increases linearly with the curing temperature T, indicating growth of crystallite grains.

III. THEORETICAL CONSIDERATIONS

B. E. Springette proposed effective medium theory that assumes insulator to be continuous medium in which spherical metal particles are randomly embedded. The simple cubic lattice model can be used for particulate system to explain the effective conductivity of the medium. As more and more metal particles are introduced, the lattice sites become more occupied in a random manner with each lattice site is associated a conductivity σ_i whose value depends upon whether the site is occupied by by metal or insulator. In this way network of electrical conductance is developed. The probability P_i that a site is occupied by metal particle is V_m/f where V_m is the volume fraction of the metal and f is the packing fraction. For simple cubic, BCC and FCC f takes values 0.528, 0.68 and 0.74 respectively[11,13-14].Assume that all conductances are equal to $\bar{\sigma}$. Let one conductance be changed to back to its true value σ_i , examine the voltage difference between the V_i and the voltage across $\sigma_i$and voltage across $\bar{\sigma}$ far from σ_i is V. the conductance of the adjacent nodes of the network of conductances$\bar{\sigma}$ = (1/2)z $\bar{\sigma}$ where z is the coordination number of the lattice. Consider such pair of nodes and consider the conductance across it, replacing the rest of the network by a conductance σ_n. If the current flowing in to the lattice is I, then all the conductances are equal to $\bar{\sigma}$, the voltage drop across the node is given by[11],

$$v = \frac{I}{(\sigma_n + \bar{\sigma})} = \bar{v}$$

There fore $\sigma_n = [\frac{1}{2}z - 1]\bar{\sigma}$ where $\bar{\sigma}$ is replaced by σ_i the voltage drop becomes,

$$v_i = \frac{I}{(\sigma_n + \sigma_i)} = \frac{v(\sigma_n + \bar{\sigma})}{(\sigma_n + \sigma_i)}$$

Substituting for $\sigma_n, v_i - \bar{v} = \bar{v}(\sigma_i - \bar{\sigma})/[\sigma_i + (\frac{1}{2}z - 1)\bar{\sigma}]$

By the definition of $\bar{\sigma}$, as all the conductances are replaced by their original values, $(v_i - \bar{v})$ should be averaged to zero. Thus if P(σ) is the probability distribution of the conductance σ, we have for the cubic network,

$$\int \frac{P(\sigma)(\sigma - \bar{\sigma})}{(\sigma + 2\bar{\sigma})} d\sigma = 0 \qquad (4)$$

where P(σ) is a binary distribution, σ_m is the metallic conductivity, σ_α is the insulator conductivity, then the above equation becomes,

$$\frac{(\frac{v_m}{f})(\sigma_m - \bar{\sigma})}{(\sigma_m + 2\sigma)} + \frac{(1 - \frac{v_m}{f})(\sigma_\alpha - \bar{\sigma})}{(\sigma_\alpha + 2\sigma)} = 0 \qquad (5)$$

This is a quadratic equation for $\bar{\sigma}$ where the root is given by,

$$4\bar{\sigma} = [\sigma_\alpha' + \sigma_m'] + [(\sigma_\alpha' + \sigma_m')^2 + 8\sigma_\alpha\sigma_m]^{1/2}$$

or the average conductivity

$$\bar{\sigma} = [\sigma_\alpha' + \sigma_m']/4 + \frac{[(\sigma_\alpha' + \sigma_m')^2 + 8\sigma_\alpha\sigma_m]^{\frac{1}{2}}}{4} \qquad (6)$$

Where,

$$\sigma_\alpha' = (2 - \frac{3v_m}{f})\sigma_\alpha \qquad (7)$$

$$\sigma_m' = (\frac{3v_m}{f} - 1)\sigma_m \qquad (8)$$

If σ_m and σ_α are known experimentally then $\sigma_m/\sigma_\alpha \approx 10^8$ we can plot a graph of $\log(\sigma_\alpha/\bar{\sigma})$ versus weight fraction or volume fraction of the metal in dielectric medium. For our experimental system SnO_2nano-particles of average size nearly 50 nm are used as continuous dielectric matrix along with glass frits of 10 μm size (10% by weight) mixed with optimized $Sb_{0.6}$:$Sn_{0.4}$ alloy particles of 5~10 μm size and varied as weight fraction w_m in the fired pastes at 800°c. For [SnO_2nano-particles +10% glass frits] the average conductivity $\sigma_\alpha = 1.4 \cdot 10^{-10}\Omega^{-1}cm^{-1}$ and the conductivity of the pure $Sb_{0.6}$:$Sn_{0.4}$ alloy $\sigma_m = 0.122\,\Omega^{-1}cm^{-1}$ for [90% $Sb_{0.6}$:$Sn_{0.4}$ + 10% glass frits] in the fired pastes.

International Journal for Research in Applied Science & Engineering Technology (IJRASET)
ISSN: 2321-9653; IC Value: 45.98; SJ Impact Factor: 6.887
Volume 6 Issue II, February 2018- Available at www.ijraset.com

IV. RESULTS AND DISCUSSIONS

As the XRD analysis show that Sno_2 and $Sb_{0.6}$:$Sn_{0.4}$alloy decomposes in to free metal and metal oxides during the firing process. The experimental values for $\sigma_\alpha$and σ_m $1.4x10^{-10}$ Ω^{-1} cm^{-1} and 0.122 Ω^{-1} cm^{-1} are used for the calculation of Log of conductivity ratio $(\sigma_\alpha/\bar{\sigma})$respectively, by using equations(6,7,8). The Springette's theoretical and experimental curves in percolation threshold differ on account of decomposition of SnO_2 and Sb:Sn alloy in to free metals Sb , Sn and their oxides during firing process as revealed by XRD analysis, wherein their relative conductivities may not remain constant (Fig.3), as model considers it for constant conductivities of $\sigma_\alpha$and σ_m for full range of weight fraction W_m in SnO_2. Also the fired films are not homogeneous and uniform in microstructure and may develop pin holes and agglomerates as revealed by SEM micrographs Fig.6(a) to 6(d). The sheet resistivity and temperature coefficient of resistance (TCR) shows similar falling trend with loading percentage of $Sb_{0.6}$:$Sn_{0.4}$alloy in SnO_2nano-particles.Theoretical and experimental comparison of log of conductivity ratio and weight fraction is shown in Fig. 3, where it is observed that theoretical percolation threshold or sudden fall in conductivity ratio is observed with the weight fraction $w_m \sim 0.3$, however experimentally the percolation is observed at $w_m \sim 0.07$. This discrepancy in the values of model prediction of percolation and observed percolation may be explained on the basis of non-spherical nature of particles and porosity of the fired polycrystalline nature of thick films as seen in the SEM micrographs. The chemical reactions occur during firing process may alter electrical conductivity of the alloy and free metal particles as revealed by XRD analysis.

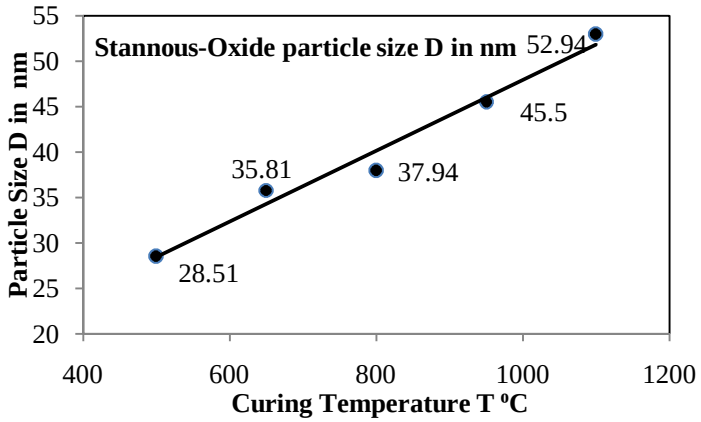

Fig.2. Variation of particle size of SnO_2 with Curing Temperature

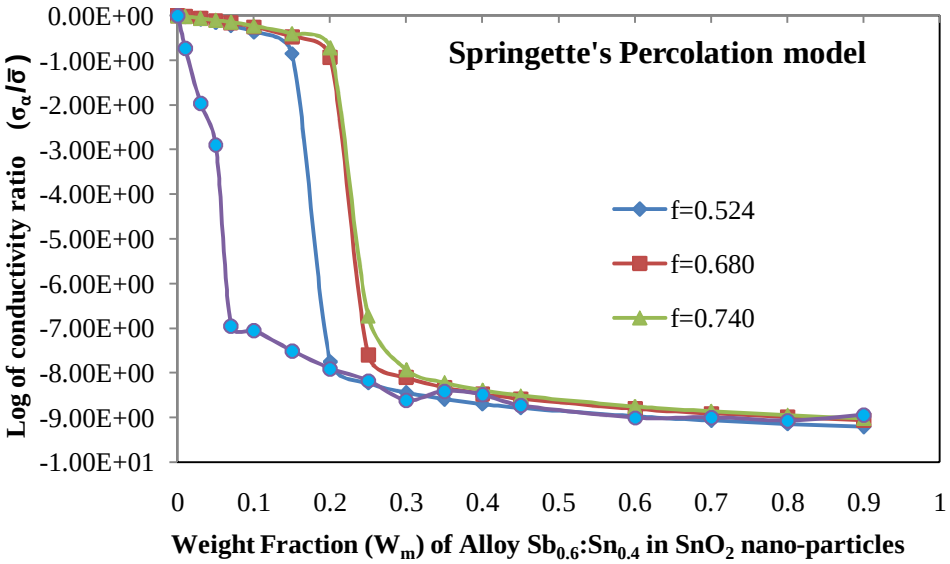

Fig. 3.The variation of electrical conductivity ratio Log $(\sigma_\alpha/\bar{\sigma})$ versus Wt.

fraction of $Sb_{0.6}$:$Sn_{0.4}$ alloy in SnO_2nano-particles along with Springette's percolation model.

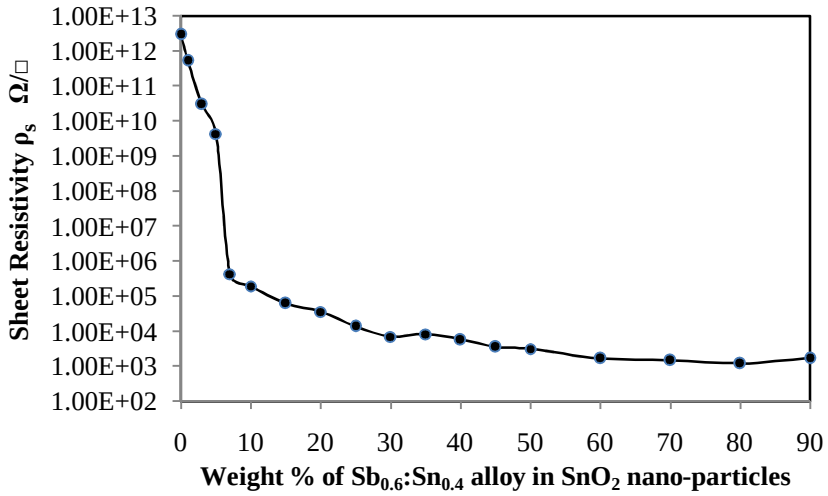

Fig. 4. The variation of electrical sheet resistivity (ρ_s) versus weight % of $Sb_{0.6}$:$Sn_{0.4}$ alloy in SnO_2nano-particles.

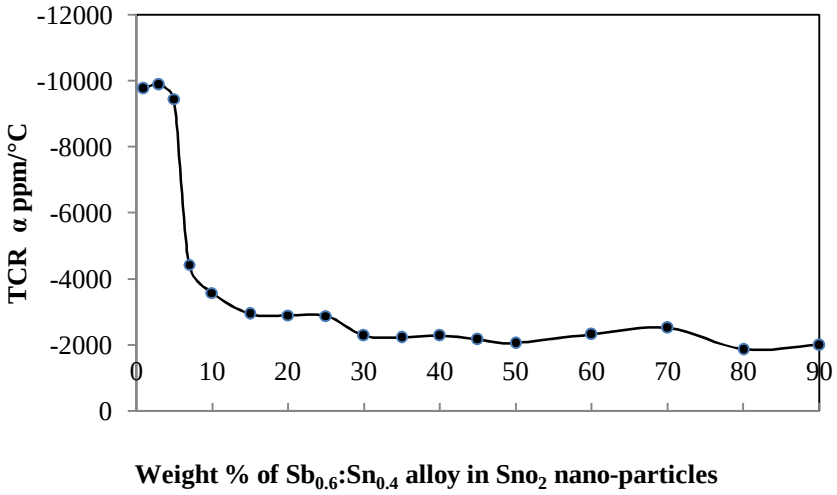

Fig. 5. The variation of Temperature coefficient of resistance (α) versus weight % of $Sb_{0.6}$:$Sn_{0.4}$ alloy in SnO_2nano-particles.

Fig. 6(a):90% Sb0.6:Sn0.4 alloy + 10% glass frits

Fig. 6(b): Pure Alumina substrate (Etched)

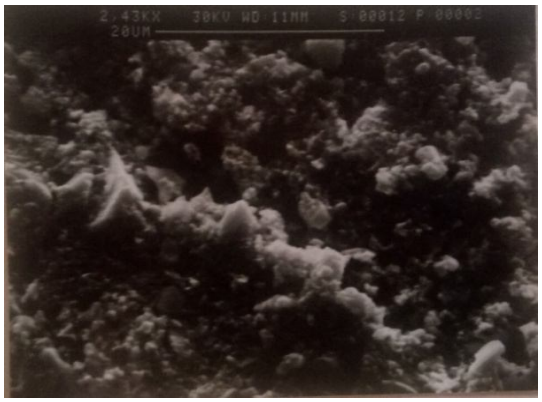

Fig. 6(c): 45%SnO_2 + 45%$Sb_{0.6}$:$Sn_{0.4}$ alloy + 10% glass

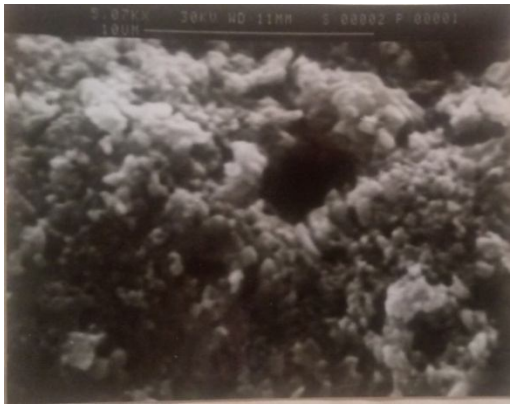

Fig. 6(d): 87% SnO_2 + 3% $Sb_{0.6}$:$Sn_{0.4}$ alloy + 10%

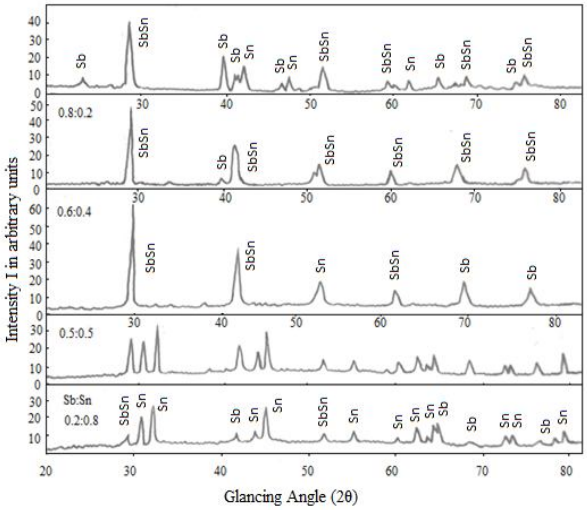

Fig. 7(a): XRD patterns of Sb:Sn alloys prepared heated at 630 ^oC .

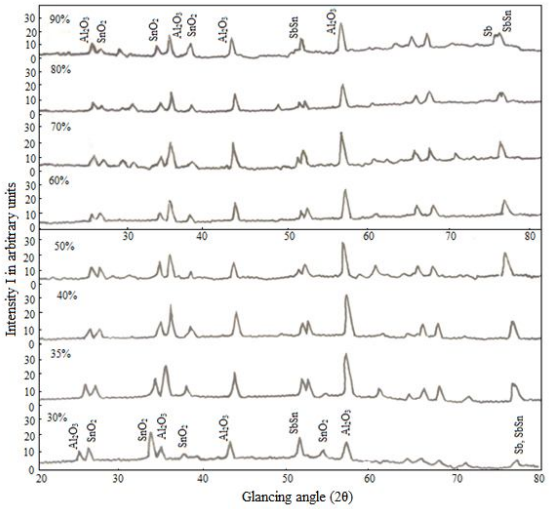

Fig. 7(b): XRD patterns of SnO_2 based $Sb_{0.6}$:$Sn_{0.4}$with different compositions alloy loaded TFRs fired at 800 ^oC

V. CONCLUSIONS

The electrical characterization of SnO_2nano-particle based thick film resistors loaded with an optimized $Sb_{0.6}$:$Sn_{0.4}$ alloy that gives minimum sheet resistivity and TCR was used to produce in the range of sheet resistivity of thick film resistors from $3x10^{12}$ Ω/□ to 1.71 k Ω/□ and TCR in the range -3145 to -814 ppm/ ^oC. Further theoretical and experimental values of percolation threshold observed at 0.2-0.3 and 0.07 weight fractions, differ on account of ideal assumptions for the Springette's effective conductivity model, wherein spherical alloy particles with constant conductivity metallic particles were supposed to be embedded in SnO_2 insulating matrix. The model needs modification for non-uniformity of microstructure and carefully designed experiments.

REFERENCES

[1] Dr K S Murthy, Short term courses on thick and thin films hybrid circuits, Sept. 1986, IISc., Bangalore,
[2] Toshio Inokuma, Y. Taketa and M Haradome, Conductive and insulative particle size effects on the electrical properties of RuO_2 thick film resisters, IEEE, 1986, Vol. CHMT-8, No. 3.
[3] Dr. K Ramkumar, Thick film deposition and processing, Short term course on thick and thin hybrid microelectronics, 1986, Bangalore.
[4] S G Ansari et al Effect of thickness on Hydrogen gas sensitivity of snO_2 nanoparticles based thick film resistors, Journal of materials science Materials in Electronics, 1996, Vol. 7, pp267-270
[5] S. G. Ansari et al The effect of humidity on an SnO_2 Thick film planar resistor, Sensors and actuators, 1994, Vol. 21(3), pp. 159-163.
[6] R Y Borse and A. S. Garde, Electrical and gas sensing properties of SnO_2 thick film resistors prepared by Screen-printing method, Sensors and Transducers, 2008,Vol.97, Issue 10, pp 64-73.

[7] S H Bhide et al, Formulation and characterization of tin oxide based resistive pastes with Sb doping, International Journal of Hybrid Microelectronics, 1988, Vol. 11, pp. 36-39.
[8] M R Kadam et al Electrical Characteristics of SnO2 –based thick film resistors loaded with $Sncl_2$, Thin Solid films, 1990, Vol. 187, Issue 2, pp. 199-208.
[9] V K Kattimani, R N Karekar R C Aiyer, Electrical properties of SnO_2:Sb based thick film resistors loaded with SbSn alloy, Int. J. Hybrid microelectronics, 1991,Vol.14.
[10] TriptiShukla, Synthesis of tin Oxide thick film and its investigation as a LPG sensor at room temperature, JST July, 2012, pp., 102-108.\
[11] B E Springette, Coductivity of a system of metallic particles dispersed in an insulated medium, Journal of Applied Physics, 1973, Vol. 44, No. 6.
[12] E R Cubellio et al., Effect of the addition of different metal oxides in lead borosilicate glasses on the electrical characteristics of SbSn composition-based thick-film resistors, Active and Passive Ele. Comp. 1993, Vol 16, pp. 7-18.
[13] F. Bucche, Electrical resistivity of conducting particles in an insulating matrix, Journal of applied Physics, 1972, Vol. 43, No. 11, pp.4837-38.
[14] A Kubovy, A percolation model of conduction threshold in thick film resistors, segregated structures, Journal of Physics, 1986, Vol. 19, No. 11, pp. 2171-83.

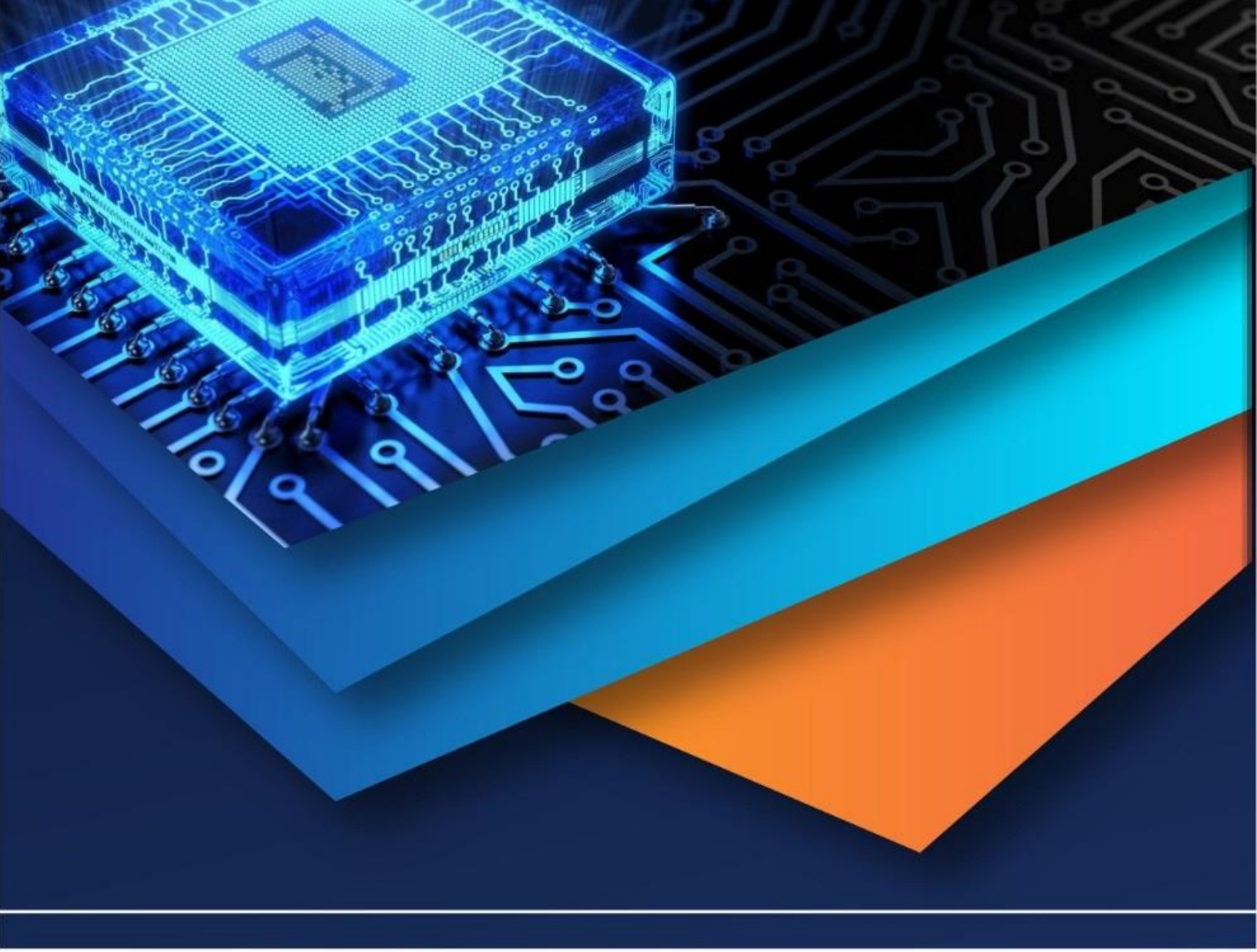

10.22214/IJRASET

45.98

IMPACT FACTOR: 7.129

IMPACT FACTOR: 7.429

INTERNATIONAL JOURNAL FOR RESEARCH

IN APPLIED SCIENCE & ENGINEERING TECHNOLOGY